Acylphosphates as versatile transient species in reaction networks and optical catalyst screenings

Andreas Englert,[1] Felix Majer, [2] Jannik L. Schiessl,[1] Alexander J. C. Kuehne,[2] and Max von Delius[1,*]

[1]Institute of Organic Chemistry, University of Ulm, 89081 Ulm Albert-Einstein-Allee 11, Germany

[2]Institute of Macromolecular and Organic Chemistry, University of Ulm, 89081 Ulm Albert-Einstein-Allee 11, Germany

*Correspondence: max.vondelius@uni-ulm.de

Abstract

Chemically-driven reaction cycles are prevalent in nature, yet artificial examples are still rare and often lack robustness or versatility. In this study, we introduce acylphosphate steady states that can be accessed from a wide range of organophosphates using either carboxylic anhydride or carbodiimide fuels. The combination of carboxylic anhydride fuel and pyridine catalysis makes this chemistry sufficiently robust to allow for 25 fueling cycles without generation of observable quantities of detrimental side products such as pyrophosphates. We demonstrate that the acylation of organophosphates gives rise to transient aggregates, and we harness the transient fluorescence of acylphosphate-bridged excimers in rapid screenings of more than 50 catalysts in a single well plate experiment. Due to its versatility and robustness, we anticipate that the organophosphate / acylphosphate reaction cycle will prove useful for the creation of chemically-driven molecular machines and transient self-assemblies.

Introduction

Non-equilibrium steady states underpin a large number of essential cellular processes. Examples range from the dissipative self-assembly of actin filaments[1] and microtubules[2] to the directed mechanical motion found in motor proteins.[3] In all these examples, nature uses enzyme catalysis and the availability or the lack of chemical fuel to enable spatial and temporal control over nontrivial functions (e.g. directed transport, mitosis, muscle contraction). To create artificial non-equilibrium steady states in the lab, typically an equilibrium between two well-defined chemical species is coupled with an exergonic process in such a way that the components of the reaction cycle act as catalysts for the transformation of a chemical fuel[4] into waste.[5, 6] Several fuel classes and building blocks for the design of artificial reaction cycles have been investigated. A first example by van Esch and co-workers explored a methyl iodide-driven reaction cycle which was used to induce the transient gelation of aryl esters.[7] More recent studies focussed on other fuels including agents for acylation,[8, 9]methylation,[10–12] and oxidation,[13–17] as well as triphosphates,[18–20] sugars,[21, 22] decarboxylating acids[23–26] and carbodiimides[27–32]. Especially, carbodiimide-driven reaction cycles, which rely on the transient formation of carboxylic anhydrides and esters attained popularity in non-enzymatic systems chemistry (Figure 1A).[33] Despite drawbacks related to *N*-acyl rearrangements and the problematic accumulation of urea waste products (H bond donor and acceptor), carbodiimides are excellent fuels, because they exhibit only minor background hydrolysis and therefore allow efficient and reliable control of reaction cycle steady states.[34] On this basis, impressive

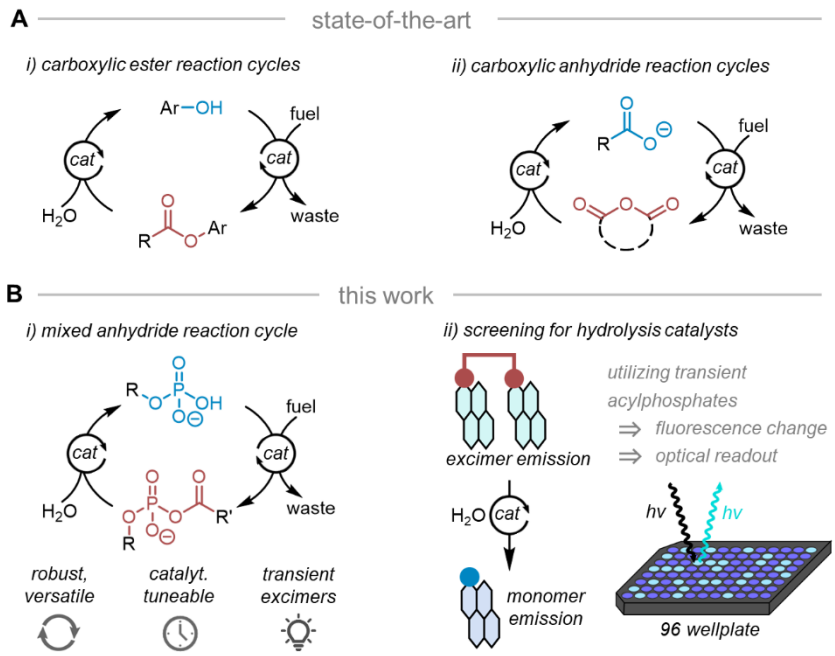

Figure 1. Overview on state-of-the-art and present work
A) State-of-the-art: relevant examples for chemically-driven, non-enzymatic reaction cycles. B) This work: scope, methodology and advantages of the organophosphate / acylphosphate reaction cycle.

feedback effects,[35] and the coupling of two reaction cycles in a thermodynamic cascade were developed.[36] Supramolecular assemblies such as vesicles,[37] microdroplets,[38] and cryptands[39] could be generated in a transient, carbodiimide-driven manner as well. However, compared to nature, where enzyme catalysis is used to assert kinetic control over the hydrolysis of otherwise inert phosphoanhydrides, few studies on artificial reaction cycles focus on catalytic control. Pioneering work by Eelkema and coworkers demonstrated how organocatalysis can be used in a beneficial way to tune the kinetics of a carboxylic ester reaction cycle.[8] We previously reported a phosphoramidate reaction cycle that exhibited exceptional kinetic control afforded by the use of 1-ethylimidazole as an organocatalyst.[40] Also, Leigh and coworkers recently showcased how chiral organocatalysts can be applied within an carboxylic anhydride reaction cycle to induce a directionally biased rotation around a C-N single bond.[41]

The design of life-like systems is also highly relevant to prebiotic chemistry and especially to the question how a possible “RNA world” arose.[42–45] A compound class, which was recently identified to be potentially of prebiotic importance, are acylphosphates.[46, 47] Specifically, these mixed phosphorus/carbon-anhydrides were applied in non-enzymatic oligoribonucleotide ligations,[48] as prebiotic phosphorylation and acylation agents,[49–51] and as aminoacyl precursors to drive peptide formation.[52, 53] Moreover, acylphosphates hold a prominent role in nature, as they serve as vital intermediates in numerous biological processes. Their significance becomes evident in various metabolic pathways, including glycolysis[54] and pyruvate metabolism.[55] Moreover, acylphosphates in the form of tRNAs are indispensable in protein biosynthesis.[56] In light of this background, and because methods for the non-enzymatic formation and for the hydrolysis of acylphosphate have been reported, [57–61] we wondered whether the two reactions could be combined under mild, preferably organocatalyzed conditions to furnish a new type of reaction cycle. Herein, we report on acylphosphates as highly versatile transient

species in chemically-driven reaction networks (Figure 1B). In proof-of-principle experiments, we demonstrate that non- equilibrium steady states from acylphosphates can give rise to transient aggregation and to the transient formation of excimers. We describe the wide scope of substrates and fuels and we propose methodology that streamlines the search for efficient hydrolysis catalysts (optical well plate screenings).

Results and Discussion

Exploration of acylphosphate formation

Acylphosphates are known to undergo hydrolysis in aqueous medium,[62] establishing an equilibrium that is shifted by several orders of magnitude towards the respective phosphate and carboxylate species. Chemically driving such a system to a non-equilibrium steady state requires high-energy reagents that react preferentially with organophosphates rather than directly with water, which potentially requires suitable catalysts. Our development of a chemically-driven acylphosphate reaction cycle therefore started with an investigation of acylation methods that are in principle feasible in dilute aqueous buffer. To ensure comparability of results, we initially focused on the acetylation of 1-naphthylphosphate (**NaphPO$_4$**). The concentrations of the substrate and the acetylated product were determined by HPLC, using an internal standard.

Table 1 depicts the highest activation yields observed within 90 minutes for different acetylation agents in the presence and absence of pyridine. Direct acetylation agents (entries 1-8) were examined first. Nearly all methods resulted in the formation of at least a limited amount of naphthalene-1-acetylphosphate (**NaphAcPO$_4$**), yet the nature of the acetylation agent is crucial for the efficiency of the process. The observed differences can be explained by the relative reactivity and the hydrolytic stability of the acylation agents. Among the reagents shown, acetyl chloride (entry 1-2) exhibits the highest reactivity and undergoes rapid nucleophilic substitution with a variety of nucleophiles including water. Background hydrolysis is therefore too fast in the case of acetyl chloride, even if pyridine was added in an attempt to favor the acylation reaction over hydrolysis via nucleophilic catalysis (entry 2).[63] By contrast, less reactive acetic anhydride gave rise to 38% **NaphAcPO$_4$** (entry 3) and to nearly quantitative conversion in the presence of pyridine (entry 4). We determined that around 66% of the anhydride is converted to the respective acylphosphate, indicating a surprisingly good fuel-to-waste efficiency of the chemical reaction cycle (Table S6). NHS-esters (entry 5-6) represent another class of acylation agents that are commonly used in aqueous environments[64] and exhibit a higher tolerance against hydrolysis, when compared to carboxylic anhydrides. Conversion to **NaphAcPO$_4$**, turned out to be quite low; however, indicating that acetic anhydride resembles a good balance of reactivity and background hydrolysis, at least for the investigated reference system. Two transacetylation experiments were conducted using acetylphosphate (entry 7-8), yet, without noticeable conversion, which is not too surprising, because the hydrolysis half-life of naphtyl-1-acetylphosphate **(NaphAcPO$_4$)** is lower compared to that of acetylphosphate (Figure S67 and S72). Remarkably, the introduction of pyridine consistently led to enhanced activation yields, underscoring the importance of organocatalysis. Other pyridine derivatives and various Lewis base catalysts were also explored and investigated within the reaction network. As can be seen in Figure S3 and Table S3, the majority of catalysts resulted in enhanced activation yields, notably with electron-deficient pyridine derivative as the most efficient ones.

Table 1: Categoric comparison of acylation methods for naphthyl-1-phosphate

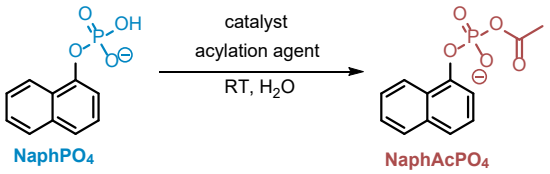

entry	pH	acylation agent	catalyst	activation yield [%]
1	7.5		none	3
2	7.5		pyridine	12
3	7.5		none	38
4	**7.5**		**pyridine**	**97**
5	7.5	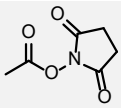	none	1
6	7.5		pyridine	6
7	7.5	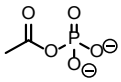	none	0
8	7.5		pyridine	0
9	7.5	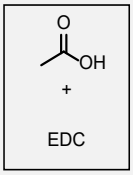	none	20
10	7.5		pyridine	40
11	5.5		none	47
12	**5.5**		**pyridine**	**81**

Reaction conditions: naphtyl-1-phosphate (25 mM), MOPS or MES buffer (250 mM), 4 equiv. of acylation agent, naphtyl-1-sulfonate as internal standard (12.5 mM), pyridine (200 mM), water as solvent.

We proceeded to investigate the indirect acylation of **NaphPO$_4$** with a combination of acetic acid and a secondary activation agent. Carbodiimides are arguably the most popular reagents for carboxylic acid activation and are frequently used in carboxylic anhydride- and ester-based reaction cycles.[33] Thus, we tested a 1:1 admixture of acetic acid and 1-ethyl-3-(3-dimethylaminopropyl)carbodiimide (EDC) at pH 7.5 and 5.5. (entries 9-12). The presence of pyridine significantly enhanced the acetylation and led to activation yields up to 81% (entry12). The experiments were conducted in a more acidic environment (i.e., pH 5.5; entries 11 and 12), since EDC activation is more effective under these conditions.[65] Other indirect acylation agents such as *N,N,N',N'*-tetramethyl-*O*-(*N*-succinimidyl)uronium hexafluorophosphate (HSTU) and di-2-pyridyldithiocarbonate (DPDTC) were also investigated, yet were found to be less effective than EDC (Table S2). Overall, the results obtained with acetic anhydride and EDC provide an ideal starting point for establishing an organophosphate / acylphosphate reaction cycle.

Optimization of system parameters and cycling experiments

Having gained preliminary insights into efficient acylation methods and the effect of nucleophilic catalysis, we shifted our attention towards the optimization of reaction parameters affecting the entire **NaphPO$_4$** / **NaphAcPO$_4$** reaction cycle (Figure 2A). Our objective was to gain a more detailed understanding and control of the system parameters. One of the most important parameters appeared to be the concentration of pyridine, which is why we monitored the system composition over time upon

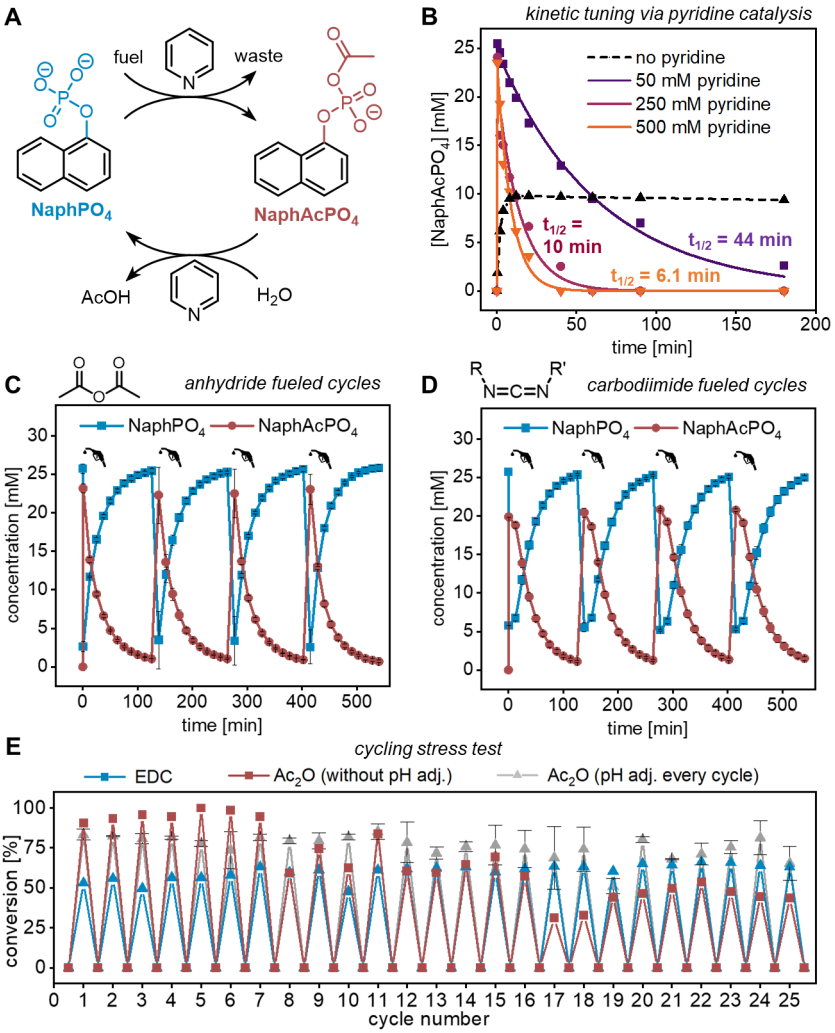

Figure 2: Optimization of NaphPO₄ reaction network

(A) Reaction scheme of **NaphPO₄** based reaction cycle. (B) Influence of Pyridine on Ac_2O-driven cycles. The determination of half-lives in the presence of pyridine was achieved by fitting the exponential decay. The dotted line serves as a visual guide. (C/D) Four consecutive fuel additions in Ac_2O/EDC-driven reaction cycles. The concentrations of **NaphAcPO₄** (red) and **NaphPO₄** (blue) were determined in triplicate using quantitative HPLC. Data points are connected to guide the eye; while error bars represent the standard deviation. Reaction conditions: naphtyl-1-phosphate (25 mM), aqueous MES or MOPS buffer (1 or 2.5 M), 4 equiv. of acylation agent per cycle, naphtyl-1-sulfonate as internal standard (12.5 mM), pyridine (200 mM). (E) Investigation of 25 consecutive fueling cycles. Conversion of **NaphPO₄** to **NaphAcPO₄** was determined 20-30s (for Ac_2O) and 2-3 min (for EDC) after fuel addition. Refueling was performed after 90% of **NaphAcPO₄** was hydrolyzed back to **NaphPO₄**. Reaction conditions: naphthyl-1-phosphate (25 mM), naphtyl-1-sulfonate as internal standard (12.5 mM), pyridine (750 mM), MOPS (1 M and 2.5 M) or acetate buffer (1 M), 3 equiv. of fuel (EDC shown in blue or Ac_2O shown in brown and grey), T = 25°C and pH = 5.5 for EDC and pH = 7.5 for Ac_2O fueling. In case of Ac_2O as fuel 6 equiv. of NaOH was also added after every cycle (grey data) to prevent a drift of pH. Error bars represent the standard deviation (triplicate execution).

addition of four equivalents of acetic anhydride (Figure 2B). As expected, we found that the pyridine concentration had a positive effect on acylphosphate formation, and only a maximum yield of 38 % for **NaphAcPO₄** was observed in the absence of pyridine. As becomes evident from Figure 2B, pyridine also has a strong effect on hydrolysis rates, which can be attributed to the fact that the acetylated pyridinium species[60, 62, 66] plays a central role in both the acyl phosphate formation and its hydrolysis (as illustrated in Scheme S1). This finding highlights an evident advantage of a reaction cycle that is subject

to (organo)catalysis, namely that the hydrolysis half-life of the transient acylphosphate can be fine-tuned from mere minutes to several hours, solely by varying the pyridine concentration. Pyridine catalysis also enables the generation of steady state mixtures under mild conditions, such as room temperature and neutral pH. Other parameters, including fuel equivalents, precursor concentration, temperature, and pH, were found to also affect the kinetics of the two reactions forming the reaction cycle and are depicted in more detail in the SI (Table S4 and S5 and Figure S4). In this context, it is worth noting that the system is robust across a broad range of parameters (even at elevated temperatures and from moderately acidic to alkaline conditions).

The system's behavior upon refueling was studied by monitoring the concentration of **NaphPO$_4$** and **NaphAcPO$_4$** during sequential additions of either acetic anhydride or EDC (Figure 2C and D). Whereas the acetic anhydride driven reaction cycle reached its **NaphAcPO$_4$** peak concentration within a few seconds, the EDC driven system required several minutes. As can also be seen from Table 1 (entry 12), the activation yield in the case of EDC was slightly lower compared to acetic anhydride. This can be attributed to a slower forward reaction, which is likely due to the additional elemental step of acid activation that makes hydrolysis (more) competitive. The hydrolysis kinetics are almost superimposable in both cases, indicating the exceptional robustness of this reaction cycle. Specifically, we found that the organophosphate **NaphPO$_4$** was fully regenerated, and no signs of pyrophosphate – as a kinetically inert side product resulting from activation of phosphorus[67, 40, 68, 69] rather than carbon – were detected by HPLC or ^{31}P-NMR spectroscopy (Figure S5 and S6). Regarding the issue of waste buildup, both the direct and indirect activation strategies, have advantages and disadvantages. On the one hand, the use of acetic anhydride is essentially free of side products, yet leads to a decrease in pH due to the release of acetic acid as a waste product. This buildup of acetic acid could potentially cause issues when performing a large number of cycles, unless it is neutralized with a base or by the presence of highly concentrated buffer systems. On the other hand, addition of EDC hydrochloride, does not alter the pH of the system significantly, but leads to *N*-acylurea byproducts[34] and to 1-ethyl-3-(3-dimethyl-aminopropyl)urea (EDU) as a terminal waste product (acetic acid is recycled in this activation mode). EDU is a strong H bond donor and H bond acceptor and it is therefore far from innocent, if transient self-assembly is the desired emergent property at steady state. As shown in Figure 2E (blue data), we were able to use EDC as fuel over 25 cycles without any noticeable fatigue of the system. When using acetic anhydride as fuel, two equivalents of acetic acid are generated during each cycle as waste. In this case, the system shows noticeable fatigue over 25 cycles (Figure 2E, red data). More well-behaved data over 25 cycles could be be obtained, if NaOH was added after every fifth (Figure S7) or after each cycle (grey data in Figure 2E).

Transient aggregation and excimer emission of pyrene-bridged acylphosphates

Having largely understood the **NaphPO$_4$** / **NaphAcPO$_4$** reaction cycle, we sought to explore functional aspects of chemically-driven acylphosphate steady states. For this reason, we turned our attention to the transient acylation of pyrene-1-phosphate (**PyrPO$_4$**). The extended π-system in **PyrPO$_4$** leads to increased lipophilicity and stronger intermolecular (i.e., π-π) interactions such that the charge reduction[70] during anhydride and/or carbodiimide fueled acetylation results in transient aggregation and phase separation of the respective product (Figure S8 and S9, Video S1 and S2). The system could

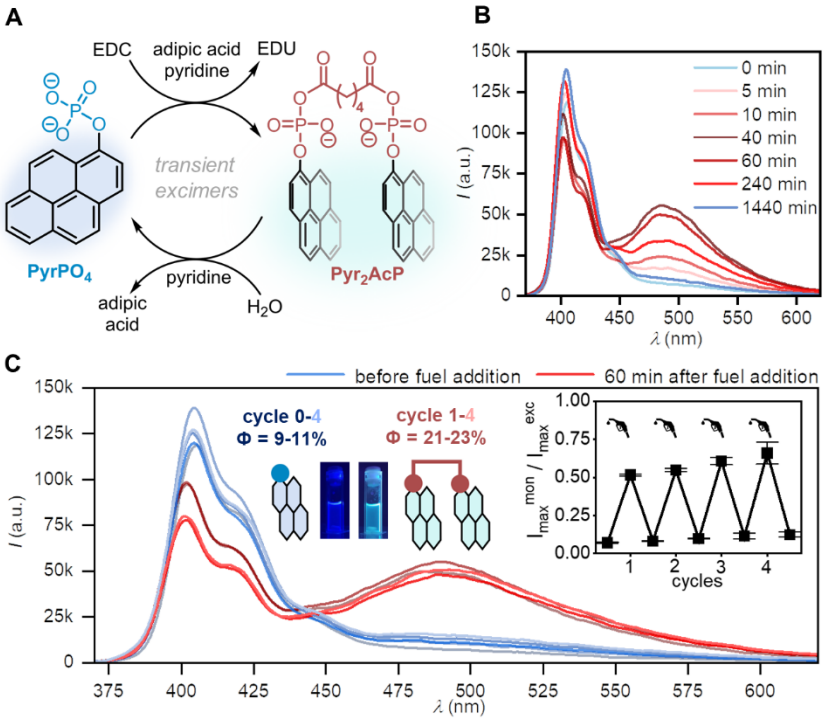

Figure 3: Fluorescence change in Pyr_2Acp non-equilibrium steady states
(A) Reaction scheme behind **$PyrPO_4$** / **Pyr_2Acp** reaction cycle. (B) Fluorescence spectra showing varying **$PyrPO_4$** / **Pyr_2Acp** non-equilibrium steady states upon addition of EDC to **$PyrPO_4$** (20 mM) and adipic acid (15 mM) (C) Photoluminescence spectra during four consecutive cycles before and 60 min after fuel addition. I_{max}^{exc} / I_{max}^{mon} presents the ratio between the intensities observed for maximal excimer and monomer emission (at 485 nm and 405 nm, respectively). Reaction conditions: 20 mM **$PyrPO_4$**, 15 mM adipic acid, 100 mM EDC, 1 M MOPS buffer, T = 25 °C, pH = 6.5, H_2O:DMF (1:1). error bars represent the standard deviation of triplicate experiments.

successfully be refueled for four times by the consecutive addition of four equivalents of fuel. Compared to **$NaphAcPO_4$**, which would hydrolyze within minutes under the standard conditions applied here (Figure S4), it is remarkable that the turbidity caused by pyrene-1-acetylphosphate (**$PyrAcPO_4$**) lasts for several hours, which could be indicative of aggregation induced negative feedback and exemplifies the utility of acylphosphate for fueled self-assemblies.[38, 71]

Because chemically-driven self-assemblies are increasingly well-established[72–75] and only few examples have been reported on transient changes in optical properties,[76–83] we decided to pursue unique opportunities that pyrenes such as **$PyrPO_4$** present in the latter arena. By employing the reaction cycle depicted in Figure 3A, we were able to establish chemically-driven excimer emission. **$PyrPO_4$** and adipic acid were used as substrates in mixed aqueous solvent (H_2O/DMF 1:1) and EDC was added as a fuel to facilitate the two-fold phosphorylation of the diacid. The resulting product **Pyr_2AcP** possesses two covalently linked pyrene moieties and displays a red-shifted fluorescence compared to the respective monomer emission. The origin of this spectral shift can be attributed to the formation of excimers, i.e. the intramolecular interaction between two pyrene moieties.

As shown in Figure 3C, we exposed this system four times to EDC fuel and monitored the emission spectra. At equilibrium, i.e. at the beginning and the end of each fuel cycle, the system exhibited near ultra-violet fluorescence between 375-450 nm, which is characteristic for the pyrene monomer. However, shortly after EDC addition, the fluorescence of the solution shifts bathochromically to sky-blue,

indicating that the **Pyr$_2$AcP** excimer is dominant at steady state (Figure S12, Video S3). Dimers or oligomers from adipic acid were not observed (HPLC-MS). Excimer emission reached its maximum after ca. 40-60 min, represented by the broad band at around 485 nm in the fluorescence spectra of Figure 3B and S10. This transient behavior is also reflected in the photoluminescence quantum yield (21-23 % after 60 minutes and 9-11 % before fuel addition, when excited at 340 nm) of the system that is continuously and predictably changing over time upon addition of the fuel (Figure S11). Over the four investigated cycles, we found that the ratio of monomer emission (I_{max}^{mon}) to excimer emission (I_{max}^{exc}) is almost invariant, see inset in the upper right corner of Figure 3C. Leaving aside the aforementioned issues with N-acylurea byproducts,[84] this good reproducibility upon refueling showcases that the acylphosphate reaction cycle is not only robust, but also highly versatile in respect to different types of emergent behavior.

Optical screening of hydrolysis catalysts

Having developed a system that exhibits distinct fluorescent properties at equilibrium and at the fuel-driven steady state, it occurred to us that transient excimers such as **Pyr$_2$AcP** could be of value for the advancement of systems chemistry. While optical readouts have been developed for biochemical investigations,[85, 86] parallel well plate screenings to report on the chemical state of a large number of chemical reaction networks are unexplored. For this reason, we isolated **Pyr$_2$AcP** and used its transient excimer emission in an optical screening setup. In the context of this present study, the following experiments served the purpose to identify further catalysts for acylphosphate hydrolysis and thus gain a broader control over acylphosphate steady state kinetics (Figure 4A). Specifically, we loaded a 96-position well plate with **Pyr$_2$AcP,** as well as a wide range of catalysts and monitored the fluorescence intensity of the excimer (at 500 nm) by the aid of a microplate reader. Since excimer emission is a specific property of the transient dimeric species, the fluorescence signal at 500 nm gradually decreases while the concentration of **Pyr$_2$AcP** diminishes. It is worth emphasizing that using a fluorescence-based response for this purpose offers two significant advantages. First, these measurements can be carried out in highly diluted media, which means that only minimal amounts of reactants are required for initial assessment. Second, and perhaps more importantly, when using a well plate setup, a large number of reactions can be monitored rapidly and continuously, because it only takes a few seconds (depending on the instrument; in our case 20 seconds) to scan the entire well plate (at 500 nm). In comparison to conventional analytical techniques commonly employed in systems chemistry such as HPLC and NMR, where a single measurement of one sample can take several minutes, a microplate reader allows measurements of the fluorescence intensity in dozens of samples within a few seconds.

As shown in Figure 4A, our well plate design included over 50 compounds that can be evaluated as potential hydrolysis catalysts with a total effort amounting to only one day of labor for one person. Following the promising results obtained with pyridine in fine-tuning the simpler **NaphPO$_4$** / **NaphAcPO$_4$** reaction cycle, this microwell plate study focused on further Lewis bases such as pyridine derivatives, imidazoles, unsaturated nitrogen-containing heterocycles, oximes, succinimides, and phosphines. Furthermore, Lewis acids such as transition metals and lanthanoid salts were included as well. A qualitative overview of the observed hydrolysis performances can be gained from the depicted heatmaps and the respective color code (Figure 4B and 4C). Dark color indicates a high fluorescence intensity at

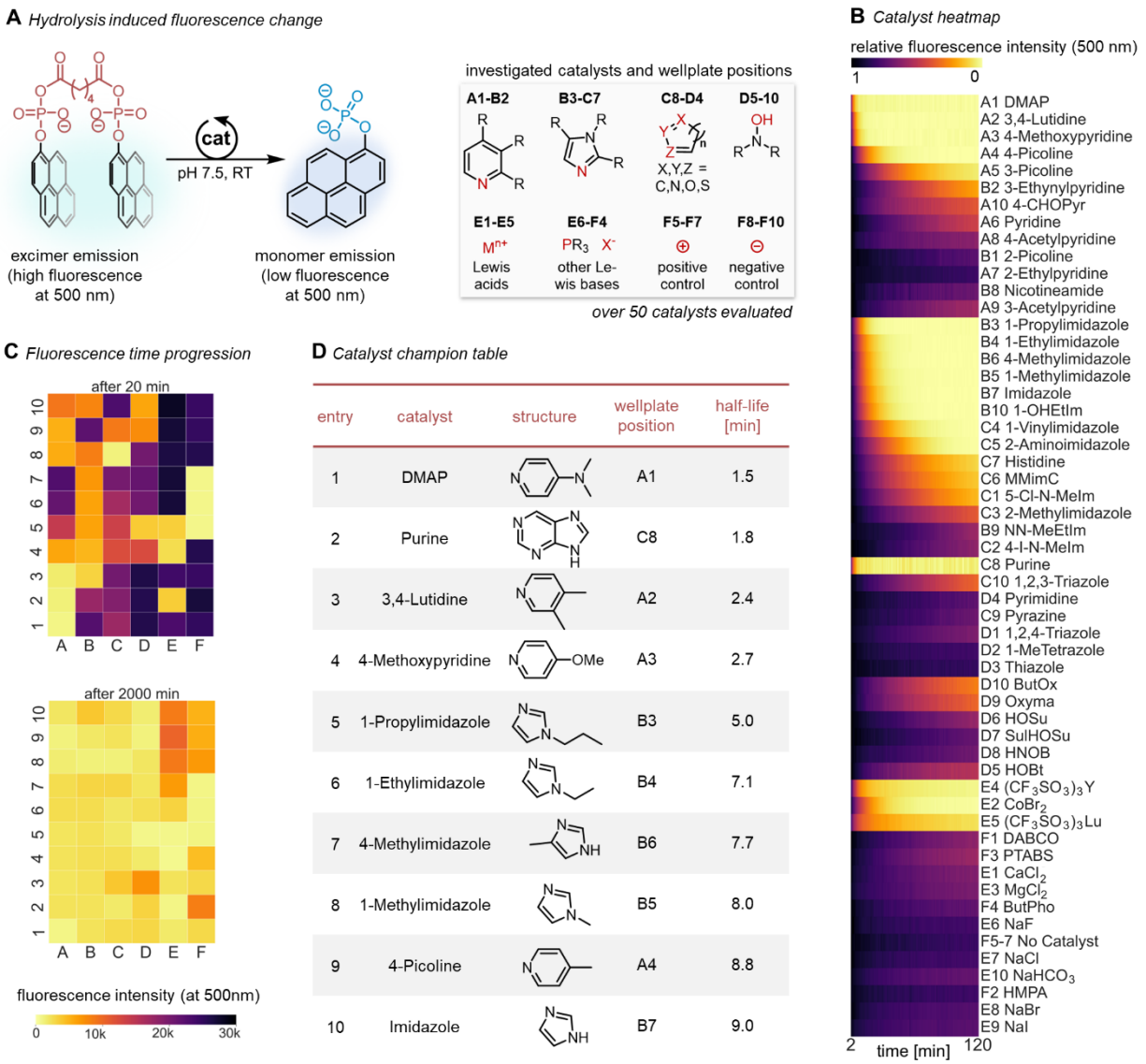

entry	catalyst	structure	wellplate position	half-life [min]
1	DMAP		A1	1.5
2	Purine		C8	1.8
3	3,4-Lutidine		A2	2.4
4	4-Methoxypyridine		A3	2.7
5	1-Propylimidazole		B3	5.0
6	1-Ethylimidazole		B4	7.1
7	4-Methylimidazole		B6	7.7
8	1-Methylimidazole		B5	8.0
9	4-Picoline		A4	8.8
10	Imidazole		B7	9.0

Figure 4: Utilizing transient fluorescence of excimer species.
(A) Reaction scheme of **Pyr$_2$AcP** hydrolysis and general structures of catalysts used in well plate design. (B) Heatmap of relative fluorescence decay for all catalysts over 120 min. Catalysts are sorted according to fastest fluorescence decay within their respective catalyst class. (C) Heatmap of fluorescence decay in the presence of various catalysts after 20 min and 2000 min. (D) Table of the ten best catalysts sorted according to shortest half-lives of fluorescence decay. Reaction conditions: 6 µM **Pyr$_2$AcP**, 10 mM catalyst, 250 mM MOPS buffer, pH = 7.5, T = 25 °C. Note: experiments with lanthanoid salts were conducted at pH 5.5 with 250 mM MES buffer for solubility reasons.

500 nm and thus a low amount of hydrolysis at this given time, whereas a bright color indicates the opposite. From the heatmap representing 20 minutes reaction time, it is evident that in some experiments hydrolysis had already gone to completion, indicating efficient catalysis (for reference see Table S8: t½ (pyridine) = 107 min and t½ (no catalyst) = 895 min). The entire time course of fluorescence decay is also depicted in the heatmap shown in Figure 4B. It is important to mention that the nature of the catalyst can also affect the optical properties of the system (e.g., due to quenching). As a result, the initial fluorescence of specific catalyst systems may be already different at the beginning of the reaction. Consequently, instead of considering the absolute fluorescence of a catalyst system at a particular point of time, we rather analyzed the relative fluorescent decay and determined the corresponding half-life through exponential curve fitting (Table S8). This approach was highly successful and reliable (see below) for gaining a rough indication of particularly effective catalysts (see champion table and

associated kinetic traces in Figure 4D and S13). From the compounds tested, *N*-alkylated imidazoles and pyridines with electron donating substituents in *meta*- or *para*-position catalyzed the hydrolysis reaction most efficiently. In particular, DMAP was found to be the catalyst giving rise to the fastest fluorescence decay ($t_{1/2}$ = 1.5 min, Table S8). Besides DMAP, 27 other compounds were identified that outcompete pyridine as hydrolysis catalysts (Table S8). To ensure that the observed decrease in fluorescence intensity was indeed indicative of enhanced hydrolysis of acylphosphates, the most promising catalysts of Figure 4D were tested as additives in our **NaphPO$_4$** reference system under HPLC monitoring as sown in Figure S59-64. As shown in Figure S60 and S64, the relatively low concentration of 10 mM DMAP was sufficient to decrease the hydrolysis half-life by a factor of 22.

Organophosphate and carboxylic anhydride scope

To evaluate whether a wide range of building blocks and fuels can be used in the acylphosphate reaction cycle, we carried out a scope study. Since DMAP was found to be an efficient acylphosphate hydrolysis agent, it was used in combination with pyridine in the reaction cycles to facilitate hydrolysis within a reasonable amount of time. As figures of merit, we determined the activation yield after two minutes for the forward reaction, i.e., how much of the organophosphate was converted to the respective acylphosphate, and the hydrolysis half-life of the backward reaction. As can be seen in Figure 5 and Table S9, the scope study included aromatic (**1,2** and **5a-c**), aliphatic (**3**) and (poly-)phosphate-based (**4, 6ab** and **7ab**) substrates. The overall conversion of the organophosphate substrate to the respective acylphosphate(s) proceeded in all cases nearly quantitatively. This finding suggests that the activation strategy applied herein can be used to acylate a wide range of organic phosphates. Furthermore, it is noteworthy that using 2-(phosphonooxy)benzoic acid as substrate intramolecular acylphosphate formation was achieved *via* transacetylation of acetic anhydride (compound **2**). In the case of anhydride fuels other than acetic anhydride, for solubility reasons, the reactions had to be conducted in a 1:1 mixture of DMF/H_2O (**5a-c**) and showed similar activation yields. Whereas the activation yields were comparable for the compounds shown, we observed pronounced differences in the hydrolysis half-lives. The relative susceptibility toward hydrolysis seems similar to that of carboxylic acid esters. Specifically, the hydrolysis rate increases if electron-withdrawing groups enhance the electrophilicity of the carbonyl group in the mixed anhydride. Therefore, aromatic substrates (such as **1** and **5a**) exhibit faster hydrolysis rates than their aliphatic counterparts (**3**) and (poly)phosphates (**4, 6a, 7a**). A related trend was also observed in the double acylation of ortho- and pyrophosphates (compounds **6** and **7**). Due to charge depletion upon acylation, the hydrolysis in the twofold acylated state is significantly faster than in the mono-acylated state. Particularly long hydrolysis half-lives were observed for compounds **2** and **5b-c**. On the one hand, this can be attributed to the fact that the reactions for compounds **5a-c** were not conducted in pure aqueous medium, but instead in a DMF-water mixture (comparison of hydrolysis half-lives of **5a**). On the other hand, the acyl phosphates **2**, **5b** and **5c** have sterically more demanding residues, which disfavors nucleophilic attack of the catalyst. Nevertheless, hydrolysis takes place in all cases, indicating that these fuels can be put to use in chemically-driven steady states.

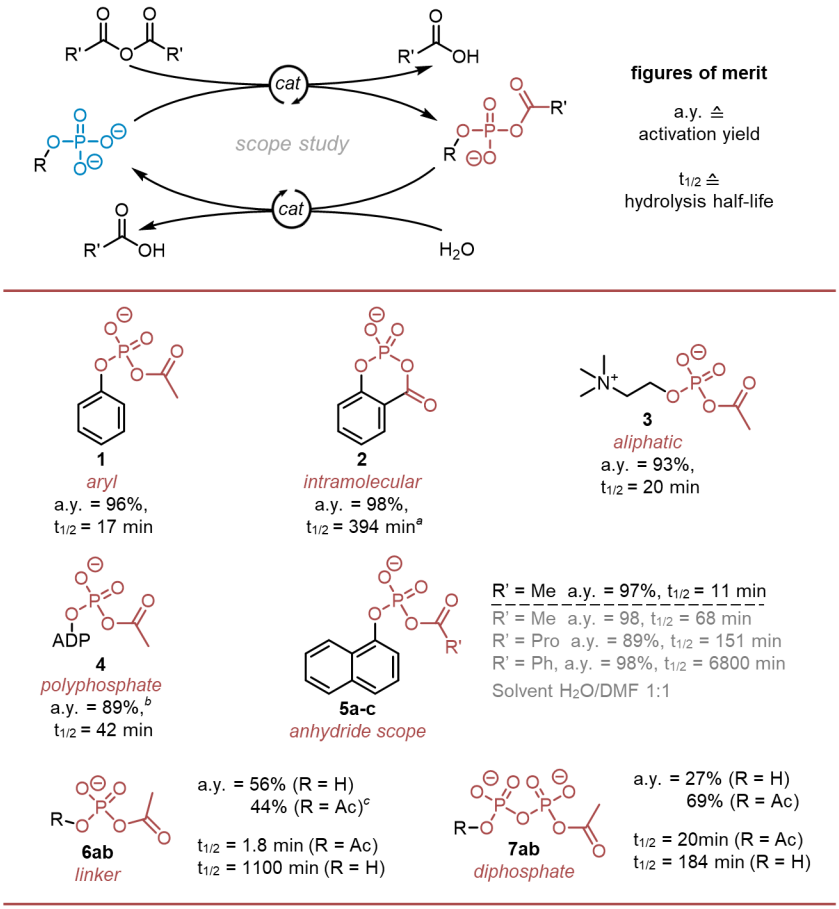

Figure 5: Scope study of acylphosphate reaction cycle
Activation yields were determined by quantitative ^{31}P-NMR spectroscopy with TMP (10 mM) as internal standard after 2 min reaction time. Hydrolysis half-lives were obtained by fitting the exponential decay. Reaction conditions: 25 mM substrate, 100 mM anhydride, 10 mM pyridine, 10 mM DMAP, 1 M MOPS buffer, pH = 7.5, T = 25°C. Notes: The reactions of acylphosphates **5b-d** were also conducted in DMF/H_2O 1:1 as solvent (data shown in grey). Kinetic data are shown in Figure S65-S76. [a]Substrate showed slight dephosphorylation over time. [b]Substrate was acylated multiple times. [c]Due to the rapid hydrolysis of compound **6a**, the activation yield determined after 2 min probably deviates from the peak concentration of this species.

Conclusion

We demonstrate that acylphosphates, the mixed anhydrides of organophosphates and carboxylates, form a robust chemical reaction cycle that can be driven by carboxylic anhydride or carbodiimide fuels. A notable difference of acylphosphates as transient species, when compared to carboxylic anhydrides, is that under the conditions typically used (pH 5-8) they are negatively charged, which we expect to be an advantage for the progressive operation of molecular machines. A significant benefit compared to the phosphoramidate reaction cycle described by us recently,[40] is that thanks to organocatalysis and activation on the electrophilic carbon atom, acylphosphates can be generated without accumulation of inert pyrophosphate side products. The use of pyridine catalysts also makes acylphosphate steady states highly tunable in respect to the kinetics of both the condensation and the hydrolysis reaction. Therefore, we were able to generate transient aggregates and excimers using this approach and carry out up to 25 fuel cycles, which compares favourably with the state of the art.[28, 87, 88] Based on these proof-of-principle results, we believe that the non-equilibrium steady states from acylphosphates will find further uses in molecular machines and dissipative self-assemblies. With the use of acylphosphate

excimers in optical catalyst screenings, we showcase powerful methodology that we expect to be broadly useful for identifying efficient catalysts reliably and in a short amount of time.

Acknowledgements

This work was supported by the European Union (ERCstg 802428 "'SUPRANET"'). The authors would like to thank Dr. Markus Lamla for assistance with fluorescence microwell plate measurements.

Author and contributions

Conceptualization: M.v.D. and A.E.; Methodology: A.E., F.M.; Investigation: A.E., J.L.S., Characterization and Resources: A.E., F.M., A.J.C.K. , J.L.S. Writing: A.E., and M.v.D.

Data availability

The datasets generated during this study are available at https://doi.org/10.5281/zenodo.10159655.

References

1. Pollard, T.D., Blanchoin, L., and Mullins, R.D. (2000). Molecular mechanisms controlling actin filament dynamics in nonmuscle cells. Annu. Rev. Biophys. 29, 545–576. 10.1146/annurev.biophys.29.1.545.

2. Brouhard, G.J., and Rice, L.M. (2018). Microtubule dynamics: an interplay of biochemistry and mechanics. Nat. Rev. Mol. Cell Biol. 19, 451–463. 10.1038/s41580-018-0009-y.

3. Schliwa, M., and Woehlke, G. (2003). Molecular motors. Nature 422, 759–765. 10.1038/nature01601.

4. We use the term "fuel" for the substrate in an exergonic process, which is coupled to the organophosphate/acylphosphate equilibrium in such a way that a non-equilibrium steady state can be sustained while fuel is present. For a semantic and technical perspective see: Aprahamian, I., and Goldup, S.M. (2023). Non-equilibrium Steady States in Catalysis, Molecular Motors, and Supramolecular Materials: Why Networks and Language Matter. J. Am. Chem. Soc. 10.1021/jacs.2c12665.

5. Ragazzon, G., and Prins, L.J. (2018). Energy consumption in chemical fuel-driven self-assembly. Nat. Nanotechnol. 13, 882–889. 10.1038/s41565-018-0250-8.

6. Borsley, S., Leigh, D.A., and Roberts, B.M.W. (2022). Chemical fuels for molecular machinery. Nat. Chem. 14, 728–738. 10.1038/s41557-022-00970-9.

7. Boekhoven, J., Brizard, A.M., Kowlgi, K.N.K., Koper, G.J.M., Eelkema, R., and van Esch, J.H. (2010). Dissipative self-assembly of a molecular gelator by using a chemical fuel. Angew. Chem. Int. Ed. 49, 4825–4828. 10.1002/anie.201001511.

8. Helm, M.P., Wang, C.-L., Fan, B., Macchione, M., Mendes, E., and Eelkema, R. (2020). Organocatalytic Control over a Fuel-Driven Transient-Esterification Network. Angew. Chem. Int. Ed. 132, 20785–20792. 10.1002/ange.202008921.

9. Wilson, M.R., Solà, J., Carlone, A., Goldup, S.M., Lebrasseur, N., and Leigh, D.A. (2016). An autonomous chemically fuelled small-molecule motor. Nature 534, 235–240. 10.1038/nature18013.

10. Boekhoven, J., Hendriksen, W.E., Koper, G.J.M., Eelkema, R., and van Esch, J.H. (2015). Transient assembly of active materials fueled by a chemical reaction. Science 349, 1075–1079. 10.1126/science.aac6103.

11. Su, B., Chi, T., Ye, Z., Xiang, Y., Dong, P., Liu, D., Addonizio, C.J., and Webber, M.J. (2023). Transient and Dissipative Host-Guest Hydrogels Regulated by Consumption of a Reactive Chemical Fuel. Angew. Chem. Int. Ed. 62, e202216537. 10.1002/anie.202216537.

12. Cheng, M., Chen, D., Zhang, L., Xiao, T., Jiang, J., and Wang, L. (2023). Chemical fuel-driven gelation with dissipative assembly-induced emission. Org. Chem. Front. 10, 1380–1385. 10.1039/D2QO01888H.

13. Leira-Iglesias, J., Sorrenti, A., Sato, A., Dunne, P.A., and Hermans, T.M. (2016). Supramolecular pathway selection of perylenediimides mediated by chemical fuels. Chem. Commun. 52, 9009–9012. 10.1039/C6CC01192F.

14. Morrow, S.M., Colomer, I., and Fletcher, S.P. (2019). A chemically fuelled self-replicator. Nat. Commun. 10, 1011. 10.1038/s41467-019-08885-9.

15. Yang, S., Schaeffer, G., Mattia, E., Markovitch, O., Liu, K., Hussain, A.S., Ottelé, J., Sood, A., and Otto, S. (2021). Chemical Fueling Enables Molecular Complexification of Self-Replicators. Angew. Chem. Int. Ed. 60, 11344–11349. 10.1002/anie.202016196.

16. Fan, B., Men, Y., Rossum, S.A.P., Li, G., and Eelkema, R. (2020). A Fuel-Driven Chemical Reaction Network Based on Conjugate Addition and Elimination Chemistry. ChemSystemsChem 2, e1900028. 10.1002/syst.201900028.

17. Selmani, S., Schwartz, E., Mulvey, J.T., Wei, H., Grosvirt-Dramen, A., Gibson, W., Hochbaum, A.I., Patterson, J.P., Ragan, R., and Guan, Z. (2022). Electrically Fueled Active Supramolecular Materials. J. Am. Chem. Soc. 144, 7844–7851. 10.1021/jacs.2c01884.

18. Heinen, L., and Walther, A. (2019). Programmable dynamic steady states in ATP-driven nonequilibrium DNA systems. Sci. Adv. 5, eaaw0590. 10.1126/sciadv.aaw0590.

19. Sorrenti, A., Leira-Iglesias, J., Sato, A., and Hermans, T.M. (2017). Non-equilibrium steady states in supramolecular polymerization. Nat. Commun. 8, 15899. 10.1038/ncomms15899.

20. Maiti, S., Fortunati, I., Ferrante, C., Scrimin, P., and Prins, L.J. (2016). Dissipative self-assembly of vesicular nanoreactors. Nat. Chem. 8, 725–731. 10.1038/nchem.2511.

21. Lu, H., Hao, J., and Wang, X. (2022). Host-Fueled Transient Supramolecular Hydrogels. ChemSystemsChem 4, e202100050. 10.1002/syst.202100050.

22. Jo, H., Selmani, S., Guan, Z., and Sim, S. (2023). Sugar-Fueled Dissipative Living Materials. J. Am. Chem. Soc. 145, 1811–1817. 10.1021/jacs.2c11122.

23. Del Giudice, D., and Di Stefano, S. (2023). Dissipative Systems Driven by the Decarboxylation of Activated Carboxylic Acids. Acc. Chem. Res. 56, 889–899. 10.1021/acs.accounts.3c00047.

24. Olivieri, E., Quintard, G., Naubron, J.-V., and Quintard, A. (2021). Chemically Fueled Three-State Chiroptical Switching Supramolecular Gel with Temporal Control. J. Am. Chem. Soc. 143, 12650–12657. 10.1021/jacs.1c05183.

25. Erbas-Cakmak, S., Fielden, S.D.P., Karaca, U., Leigh, D.A., McTernan, C.T., Tetlow, D.J., and Wilson, M.R. (2017). Rotary and linear molecular motors driven by pulses of a chemical fuel. Science 358, 340–343. 10.1126/science.aao1377.

26. Ghosh, A., Paul, I., Adlung, M., Wickleder, C., and Schmittel, M. (2018). Oscillating Emission of 2Rotaxane Driven by Chemical Fuel. Org. Lett. 20, 1046–1049. 10.1021/acs.orglett.7b03996.

27. Borsley, S., Leigh, D.A., and Roberts, B.M.W. (2021). A Doubly Kinetically-Gated Information Ratchet Autonomously Driven by Carbodiimide Hydration. J. Am. Chem. Soc. 143, 4414–4420. 10.1021/jacs.1c01172.

28. Chen, X., Stasi, M., Rodon-Fores, J., Großmann, P.F., Bergmann, A.M., Dai, K., Tena-Solsona, M., Rieger, B., and Boekhoven, J. (2023). A Carbodiimide-Fueled Reaction Cycle That Forms Transient 5(4H)-Oxazolones. J. Am. Chem. Soc. 145, 6880–6887. 10.1021/jacs.3c00273.

29. Kariyawasam, L.S., and Hartley, C.S. (2017). Dissipative Assembly of Aqueous Carboxylic Acid Anhydrides Fueled by Carbodiimides. J. Am. Chem. Soc. 139, 11949–11955. 10.1021/jacs.7b06099.

30. Würbser, M.A., Schwarz, P.S., Heckel, J., Bergmann, A.M., Walther, A., and Boekhoven, J. (2021). Chemically Fueled Block Copolymer Self-Assembly into Transient Nanoreactors. ChemSystemsChem 3, e2100015. 10.1002/syst.202100015.

31. Mo, K., Zhang, Y., Dong, Z., Yang, Y., Ma, X., Feringa, B.L., and Zhao, D. (2022). Intrinsically unidirectional chemically fuelled rotary molecular motors. Nature 609, 293–298. 10.1038/s41586-022-05033-0.

32. Zhang, Y., Chang, Z., Zhao, H., Crespi, S., Feringa, B.L., and Zhao, D. (2020). A Chemically Driven Rotary Molecular Motor Based on Reversible Lactone Formation with Perfect Unidirectionality. Chem 6, 2420–2429. 10.1016/j.chempr.2020.07.025.

33. Schwarz, P.S., Tena-Solsona, M., Dai, K., and Boekhoven, J. (2022). Carbodiimide-fueled catalytic reaction cycles to regulate supramolecular processes. Chem. Commun. 58, 1284–1297. 10.1039/D1CC06428B.

34. Williams, A., and Ibrahim, I.T. (1981). Carbodiimide chemistry: recent advances. Chem. Rev. 81, 589–636. 10.1021/cr00046a004.

35. Bal, S., Das, K., Ahmed, S., and Das, D. (2019). Chemically Fueled Dissipative Self-Assembly that Exploits Cooperative Catalysis. Angew. Chem. Int. Ed. 58, 244–247. 10.1002/anie.201811749.

36. Liu, K., Blokhuis, A.W.P., Dijt, S.J., Hamed, S., Kiani, A., Matysiak, B.M., and Otto, S. (2022). Systems Chemistry across Multiple Length Scales: Macroscopic Flow via Dissipative Co-Assemblies Featuring Transient Amides ChemRxiv. 10.26434/chemrxiv-2022-msgf8

37. Wanzke, C., Jussupow, A., Kohler, F., Dietz, H., Kaila, V.R.I., and Boekhoven, J. (2020). Dynamic Vesicles Formed By Dissipative Self-Assembly. ChemSystemsChem 2, e1900044. 10.1002/syst.201900044.

38. Tena-Solsona, M., Wanzke, C., Riess, B., Bausch, A.R., and Boekhoven, J. (2018). Self-selection of dissipative assemblies driven by primitive chemical reaction networks. Nat. Commun. 9, 2044. 10.1038/s41467-018-04488-y.

39. Hossain, M.M., Jayalath, I.M., Baral, R., and Hartley, C.S. (2022). Carbodiimide-Induced Formation of Transient Polyether Cages. ChemSystemsChem 4, e202200016. 10.1002/syst.202200016.

40. Englert, A., Vogel, J.F., Bergner, T., Loske, J., and Delius, M. von (2022). A Ribonucleotide ↔ Phosphoramidate Reaction Network Optimized by Computer-Aided Design. J. Am. Chem. Soc. 144, 15266–15274. 10.1021/jacs.2c05861.

41. Borsley, S., Kreidt, E., Leigh, D.A., and Roberts, B.M.W. (2022). Autonomous fuelled directional rotation about a covalent single bond. Nature 604, 80–85. 10.1038/s41586-022-04450-5.

42. Miljanić, O.Š. (2017). Small-Molecule Systems Chemistry. Chem 2, 502–524. 10.1016/j.chempr.2017.03.002.

43. Ruiz-Mirazo, K., Briones, C., and La Escosura, A. de (2014). Prebiotic systems chemistry: new perspectives for the origins of life. Chem. Rev. 114, 285–366. 10.1021/cr2004844.

44. Sutherland, J.D. (2016). The Origin of Life--Out of the Blue. Angew. Chem. Int. Ed. 55, 104–121. 10.1002/anie.201506585.

45. Szostak, J.W. (2017). The Narrow Road to the Deep Past: In Search of the Chemistry of the Origin of Life. Angew. Chem. Int. Ed. 56, 11037–11043. 10.1002/anie.201704048.

46. Biron, J.-P., and Pascal, R. (2004). Amino acid N-carboxyanhydrides: activated peptide monomers behaving as phosphate-activating agents in aqueous solution. J. Am. Chem. Soc. 126, 9198–9199. 10.1021/ja048189s.

47. Biron, J.-P., Parkes, A.L., Pascal, R., and Sutherland, J.D. (2005). Expeditious, potentially primordial, aminoacylation of nucleotides. Angew. Chem. Int. Ed. 44, 6731–6734. 10.1002/anie.200501591.

48. Bowler, F.R., Chan, C.K.W., Duffy, C.D., Gerland, B., Islam, S., Powner, M.W., Sutherland, J.D., and Xu, J. (2013). Prebiotically plausible oligoribonucleotide ligation facilitated by chemoselective acetylation. Nat. Chem. 5, 383–389. 10.1038/nchem.1626.

49. Whicher, A., Camprubi, E., Pinna, S., Herschy, B., and Lane, N. (2018). Acetyl Phosphate as a Primordial Energy Currency at the Origin of Life. Orig. Life Evol. Biosph. 48, 159–179. 10.1007/s11084-018-9555-8.

50. Bonfio, C., Caumes, C., Duffy, C.D., Patel, B.H., Percivalle, C., Tsanakopoulou, M., and Sutherland, J.D. (2019). Length-Selective Synthesis of Acylglycerol-Phosphates through Energy-Dissipative Cycling. J. Am. Chem. Soc. 141, 3934–3939. 10.1021/jacs.8b12331.

51. Werner, E., Pinna, S., Mayer, R.J., and Moran, J. (2023). Metal/ADP Complexes Promote Phosphorylation of Ribonucleotides. J. Am. Chem. Soc. 145, 21630–21637. 10.1021/jacs.3c08047.

52. Dai, K., Pol, M., Saile, L., Sharma, A., Liu, B., Thomann, R., Trefs, J., Qiu, D., Moser, S., Wiesler, S., Balzer, B., Hugel, T., Jessen, H., Pappas, C. (2023). Systems chemistry of aminoacyl phosphates: Spontaneous and selective peptide oligomerisation in water driven by phase changes. ChemRxiv. 10.26434/chemrxiv-2023-lg3cw.

53. Weber, A.L., and Orgel, L.E. (1978). The formation of peptides from the 2'(3')-glycyl ester of a nucleotide. J. Mol. Evol. 11, 189–198. 10.1007/BF01734480.

54. Bodner, G.M. (1986). Metabolism Part I: Glycolysis for the Embden-Meyerhoff pathway. J. Chem. Educ. 63, 566. 10.1021/ed063p566.

55. McCleary, W.R., Stock, J.B., and Ninfa, A.J. (1993). Is acetyl phosphate a global signal in Escherichia coli? J. Bacteriol. 175, 2793–2798. 10.1128/jb.175.10.2793-2798.1993.

56. Lengyel, P., and Söll, D. (1969). Mechanism of protein biosynthesis. Bacteriol. rev. 33, 264–301. 10.1128/br.33.2.264-301.1969.

57. Kluger, R., Loo, R.W., and Mazza, V. (1997). Biomimetically Activated Amino Acids. Catalysis in the Hydrolysis of Alanyl Ethyl Phosphate. J. Am. Chem. Soc. 119, 12089–12094. 10.1021/ja972406q.

58. Lacey, J.C., Senaratne, N., and Mullins, D.W. (1984). Hydrolytic properties of phenylalanyl- and N-acetylphenylalanyl adenylate anhydrides. Orig. Life Evol. Biosph. 15, 45–54. 10.1007/BF01809392.

59. Kluger, R., and Cameron, L.L. (2002). Activation of acyl phosphate monoesters by lanthanide ions: enhanced reactivity of benzoyl methyl phosphate. J. Am. Chem. Soc. 124, 3303–3308. 10.1021/ja016600v.

60. Avison, A.W.D. (1955). The synthesis of acyl phosphates in aqueous solution. J. Chem. Soc., 732. 10.1039/JR9550000732.

61. Crans, D.C., and Whitesides, G.M. (1983). A convenient synthesis of disodium acetyl phosphate for use in in situ ATP cofactor regeneration. J. Org. Chem. 48, 3130–3132. 10.1021/jo00166a048.

62. Di Sabato, G., and Jencks, W.P. (1961). Mechanism and Catalysis of Reactions of Acyl Phosphates. II. Hydrolysis 1. J. Am. Chem. Soc. 83, 4400–4405. 10.1021/ja01482a025.

63. Bentley, T.W., Llewellyn, G., and McAlister, J.A. (1996). S(N)2 Mechanism for Alcoholysis, Aminolysis, and Hydrolysis of Acetyl Chloride. J. Org. Chem. 61, 7927–7932. 10.1021/jo9609844.

64. Koniev, O., and Wagner, A. (2015). Developments and recent advancements in the field of endogenous amino acid selective bond forming reactions for bioconjugation. Chem. Soc. Rev. 44, 5495–5551. 10.1039/C5CS00048C.

65. Nakajima, N., and Ikada, Y. (1995). Mechanism of amide formation by carbodiimide for bioconjugation in aqueous media. Bioconjug. Chem. 6, 123–130. 10.1021/bc00031a015.

66. Fischer, C.B., Xu, S., and Zipse, H. (2006). Steric effects in the uncatalyzed and DMAP-catalyzed acylation of alcohols-quantifying the window of opportunity in kinetic resolution experiments. Chem. Eur. J. 12, 5779–5784. 10.1002/chem.200600280.

67. Röthlingshöfer, M., Kervio, E., Lommel, T., Plutowski, U., Hochgesand, A., and Richert, C. (2008). Chemical primer extension in seconds. Angew. Chem. Int. Ed. 47, 6065–6068. 10.1002/anie.200801260.

68. Sun, J., Vogel, J., Chen, L., Schleper, A.L., Bergner, T., Kuehne, A.J.C., and Delius, M. von (2022). Carbodiimide-Driven Dimerization and Self-Assembly of Artificial, Ribose-Based Amphiphiles. Chem. Eur. J. 28, e202104116. 10.1002/chem.202104116.

69. Wright, T.H., Giurgiu, C., Zhang, W., Radakovic, A., O'Flaherty, D.K., Zhou, L., and Szostak, J.W. (2019). Prebiotically Plausible "Patching" of RNA Backbone Cleavage through a 3'-5' Pyrophosphate Linkage. J. Am. Chem. Soc. 141, 18104–18112. 10.1021/jacs.9b08237.

70. Rieß, B., Grötsch, R.K., and Boekhoven, J. (2020). The Design of Dissipative Molecular Assemblies Driven by Chemical Reaction Cycles. Chem 6, 552–578. 10.1016/j.chempr.2019.11.008.

71. Kriebisch, C.M.E., Bergmann, A.M., and Boekhoven, J. (2021). Fuel-Driven Dynamic Combinatorial Libraries. J. Am. Chem. Soc. 143, 7719–7725. 10.1021/jacs.1c01616.

72. De, S., and Klajn, R. (2018). Dissipative Self-Assembly Driven by the Consumption of Chemical Fuels. Adv. Mater. 30, e1706750. 10.1002/adma.201706750.

73. Das, K., Gabrielli, L., and Prins, L.J. (2021). Chemically Fueled Self-Assembly in Biology and Chemistry. Angew. Chem. Int. Ed. 60, 20120–20143. 10.1002/anie.202100274.

74. Chen, X., Würbser, M.A., and Boekhoven, J. (2023). Chemically Fueled Supramolecular Materials. Acc. Mater. Res. 4, 416–426. 10.1021/accountsmr.2c00244.

75. Della Sala, F., Neri, S., Maiti, S., Chen, J.L.-Y., and Prins, L.J. (2017). Transient self-assembly of molecular nanostructures driven by chemical fuels. Curr. Opin. Biotechnol. 46, 27–33. 10.1016/j.copbio.2016.10.014.

76. Zong, Z., Zhang, Q., Qiu, S.-H., Wang, Q., Zhao, C., Zhao, C.-X., Tian, H., and Qu, D.-H. (2022). Dynamic Timing Control over Multicolor Molecular Emission by Temporal Chemical Locking. Angew. Chem. Int. Ed. 61, e202116414. 10.1002/anie.202116414.

77. Stasi, M., Monferrer, A., Babl, L., Wunnava, S., Dirscherl, C.F., Braun, D., Schwille, P., Dietz, H., and Boekhoven, J. (2022). Regulating DNA-Hybridization Using a Chemically Fueled Reaction Cycle. J. Am. Chem. Soc. 144, 21939–21947. 10.1021/jacs.2c08463.

78. Spatola, E., Rispoli, F., Del Giudice, D., Cacciapaglia, R., Casnati, A., Marchiò, L., Baldini, L., and Di Stefano, S. (2021). Dissipative control of the fluorescence of a 1,3-dipyrenyl calix4arene in the cone conformation. Org. Biomol. Chem. 20, 132–138. 10.1039/D1OB02096J.

79. Sonu, K.P., Dhiman, S., Garg, A., Selvakumar, D., George, S.J., and Eswaramoorthy, M. (2023). Temporally programmed switching of functional states in polyaniline film. APL Mater. 11, 31111. 10.1063/5.0140078.

80. Pezzato, C., and Prins, L.J. (2015). Transient signal generation in a self-assembled nanosystem fueled by ATP. Nat. Commun. 6, 7790. 10.1038/ncomms8790.

81. Cardona, M.A., Chen, R., Maiti, S., Fortunati, I., Ferrante, C., Gabrielli, L., Das, K., and Prins, L.J. (2020). Time-gated fluorescence signalling under dissipative conditions. Chem. Commun. 56, 13979–13982. 10.1039/D0CC05993E.

82. Cheng, M., Chen, D., Zhang, L., Xiao, T., Jiang, J., and Wang, L. (2023). Chemical fuel-driven gelation with dissipative assembly-induced emission. Org. Chem. Front. 10, 1380–1385. 10.1039/D2QO01888H.

83. Della Sala, F., Maiti, S., Bonanni, A., Scrimin, P., and Prins, L.J. (2018). Fuel-Selective Transient Activation of Nanosystems for Signal Generation. Angew. Chem., Int. Ed. 57, 1611–1615. 10.1002/anie.201711964.

84. In contrast to the reference system described above, the (di)acid was used as a linker moiety and was therefore not used in excess, since otherwise only the monosubstituted product would be obtained. Under these diluted conditions the formation of N-acyl rearrangement products was observed by HPLC which could result in an efficiency loss upon cycling the system for many times.

85. Gless, B.H., Schmied, S.H., Bejder, B.S., and Olsen, C.A. (2023). Förster Resonance Energy Transfer Assay for Investigating the Reactivity of Thioesters in Biochemistry and Native Chemical Ligation. J. Am. Chem. Soc. 3, 1443–1451. 10.1021/jacsau.3c00095.

86. Aparin, I.O., Proskurin, G.V., Golovin, A.V., Ustinov, A.V., Formanovsky, A.A., Zatsepin, T.S., and Korshun, V.A. (2017). Fine Tuning of Pyrene Excimer Fluorescence in Molecular Beacons by Alteration of the Monomer Structure. J. Org. Chem. 82, 10015–10024. 10.1021/acs.joc.7b01451.

87. Singh, N., Lainer, B., Formon, G.J.M., Piccoli, S. de, and Hermans, T.M. (2020). Re-programming Hydrogel Properties Using a Fuel-Driven Reaction Cycle. J. Am. Chem. Soc. 142, 4083–4087. 10.1021/jacs.9b11503.

88. Barpuzary, D., Hurst, P.J., Patterson, J.P., and Guan, Z. (2023). Waste-Free Fully Electrically Fueled Dissipative Self-Assembly System. J. Am. Chem. Soc. 145, 3727–3735. 10.1021/jacs.2c13140.